

1 **Uranium diffusion and time-dependent adsorption–desorption in soil:**
2 **a model and experimental testing of the model**

3 J. DARMOVZALOVA^a, A. BOGHI^{a,b}, W. OTTEN^a, L. J. EADES^c, T. ROOSE^b & G. J. D. KIRK^a

4 ^a*School of Water, Energy & Environment, Cranfield University, Cranfield, Bedford MK43 0AL,*
5 *UK, ^bFaculty of Engineering and Environment, University of Southampton, Southampton SO17*
6 *1BJ, UK, and ^cSchool of Chemistry, University of Edinburgh, Edinburgh EH9 3FJ, UK*

7 **Correspondence:** Guy Kirk. E-mail: g.kirk@cranfield.ac.uk

8 **Running title:** Uranium diffusion

9

10 **Summary**

11 Most past research on uranium (U) transport and reaction in the environment has been concerned
12 with groundwater contamination, and not with uptake by plants or soil biota, both of which operate
13 over much smaller time and distance scales. We developed and tested a model of U diffusion and
14 reaction in soil at scales appropriate for uptake by plant roots, based on a model we developed in an
15 earlier paper. The model allows for the speciation of U with hydroxyl, carbonate and organic
16 ligands in the soil solution, and the nature and kinetics of sorption reactions with the soil solid. The
17 model predictions were compared with experimentally-measured concentration-distance profiles of
18 U in soil adjusted to different pHs and CO₂ pressures. Excellent agreement between observed and
19 predicted profiles was obtained using model input parameters measured or otherwise estimated
20 independently of the concentration-distance profiles, showing that the model was a correct
21 description of the system and all important processes were allowed for. The importance of the
22 kinetics of U adsorption and desorption on the time-scale of diffusion through the soil is
23 highlighted. The results are discussed in terms of the uptake of U by plant root systems, as modelled
24 in the earlier paper.

25 **Highlights**

- 26 • We developed a model of U diffusion and reaction in soil on scales relevant to uptake by plant
27 roots.
- 28 • We tested the model against measured diffusion profiles and obtained excellent agreement.
- 29 • The kinetics of U adsorption–desorption reactions are important.
- 30 • Reaction kinetics measured in shaken suspensions or flow-through systems are likely to be
31 misleading.

32

33 **Introduction**

34 Soil contamination with uranium (U) occurs from geological deposits, metal mining, nuclear waste
35 and depleted U in weapons, and it enters the food chain largely with uptake by plants from soil.
36 Understanding the mechanisms of plant uptake is difficult because of the complex biogeochemistry
37 of U in soil and the involvement of complex root–soil interactions (Mitchell *et al.*, 2013). Simple
38 empirical models exist, based on soil–plant transfer functions, but are only useful for the conditions
39 in which they have been calibrated. Most mechanistic modelling of U in the environment has been
40 concerned with groundwater contamination, and therefore with (a) much larger scales than for root
41 uptake and (b) mass flow-dominated transport, whereas U uptake by roots is generally diffusion-
42 limited (next paragraph). In an earlier paper (Boghi *et al.*, 2018) we developed a model of U uptake
43 by plants allowing for transport through soil to root surfaces, root-induced changes in the soil
44 affecting U mobility and rates of transport across the root–soil boundary. We compared the model’s
45 predictions with published information on uptake rates under different soil conditions, but did not
46 test it rigorously against experiments. In this paper we provide such a rigorous testing.

47 Simple calculations show that rates of uptake are typically far greater than can be explained by
48 mass flow alone, given typical U concentrations in soil solutions and water inflow into roots. Table
49 S1 (Supporting Information) gives such calculations for U uptake by ryegrass (*Lolium perenne* L) in
50 a range of soils, based on data of Duquène *et al.* (2010). This suggests that uptake is limited by
51 diffusion through the soil, and therefore that transport across the soil–root boundary is sufficiently
52 fast that a depletion zone develops around the root, through which U diffuses. Uranium uptake is
53 enhanced where roots are colonized by mycorrhizal fungi, although root–shoot translocation is then
54 often impeded (Davies *et al.*, 2015). Uptake into mycorrhiza must also be limited by diffusion
55 through the soil.

56 Uranium is present in soil solutions and is taken up from these by roots as the uranyl (UO_2^{2+})
57 cation and as complexes with carbonate (CO_3^{2-}) and organic (L^-) ligands (Figure 1). The complexes
58 are differentially sorbed on soil surfaces, and the extent of sorption as well as the proportions of the
59 different complexes in solution are functions of pH and CO_2 pressure, such that the sorption–pH
60 relation is bell-shaped with a peak around neutral pH but shifting to lower pH with increasing CO_2
61 pressure (Davis *et al.*, 2004; Geckeis *et al.*, 2013; Mitchell *et al.*, 2013). Therefore, diffusion
62 through the soil solution to absorbing roots might be sensitive to the changes in rhizosphere pH and
63 CO_2 pressure that are commonly caused by roots. Further, the interchange of U between the soil
64 solid and solution may be rate-limiting. Experiments on sorption kinetics in soils and sediments
65 generally show desorption of U is initially fast, but then continues at a much slower rate for some
66 weeks (Braithwaite *et al.*, 1997; Qafoku *et al.*, 2005; Handley-Sidhu *et al.*, 2009; Stoliker *et al.*,
67 2013). The model of Boghi *et al.* (2018) predicts that such time-dependency should be important on

68 the time-scale of U uptake by plant roots. The rate-limiting step is likely to be slow access to or
69 from sorption sites within soil aggregates by diffusion in the intra-aggregate pore space, rather than
70 slow chemical reactions as such (Nye & Staunton, 1994; Ptashnyk *et al.*, 2010). However the
71 available data on sorption kinetics is mainly from shaken suspension experiments in which sorption
72 is accelerated by convection and disaggregation of the soil, or from breakthrough curves in flow-
73 through systems, in which sorption is also accelerated by convection (Qafoku *et al.*, 2005; Stoliker
74 *et al.*, 2013).

75 In this paper we test Boghi *et al.*'s (2018) model against experimentally measured rates of U
76 diffusion through soil under different pHs and CO₂ pressures. We measured the diffusion of U
77 between two half-cells of soil, one of which initially contained U and the other not. From the
78 concentration-distance profiles we gauged rates of desorption in the source cell and adsorption in
79 the sink cell. We made experiments in soils adjusted to different pHs and CO₂ pressures in the
80 ranges in which U mobility is expected to be large. We compared the measured profiles with the
81 predictions of Boghi *et al.*'s (2018) model, reformulated for the planar geometry and boundary
82 conditions of the experiments. We also measured the diffusion of non-adsorbed Br⁻ ions in our half-
83 cell experimental system to determine the soil diffusion coefficient in the absence of sorption and to
84 confirm that the system behaved as expected from theory.

85 **Theory**

86 *Uranium diffusion and reaction*

87 In our experimental system, two half-cells of soil are placed in contact, one containing U and the
88 other not, and the cells are incubated so that U diffuses from the U-containing cell to the other.
89 After suitable intervals, concentration-distance profiles through the soil are determined. The
90 continuity equation for diffusion and reaction is:

$$\frac{\partial C}{\partial t} = \frac{\partial}{\partial x} \left(D \frac{\partial C}{\partial x} \right), \quad (1)$$

91 where C is the concentration of U in the whole soil and D is its diffusion coefficient in the soil,
92 given by

$$D = D_L \theta f \frac{dC_L}{dC} \quad (2)$$

93 where D_L is the diffusion coefficient in free solution, θ is the soil volumetric moisture content, f is
94 an impedance factor and C_L is the concentration of U species (free and complexed) in the soil
95 solution. The boundary conditions are

$$\begin{aligned} C = C_1 \quad x < 0 \quad C = C_0 \quad x > 0 \quad t = 0, \\ C = C_1 \quad x = -\infty \quad C = C_0 \quad x = \infty \quad t \geq 0, \end{aligned} \quad (3)$$

96 where C_1 is the concentration in the source cell, C_0 is the concentration in the sink cell ($= 0$), $x = 0$
 97 is the inter-cell boundary and $x = \infty$ is the semi-infinite far-field boundary.

98 Boghi *et al.* (2018) define two types of U in the soil solid consistent with past work on sorption
 99 kinetics (references in Introduction): one that exchanges effectively instantaneously with U species
 100 in the soil solution and one that exchanges more slowly. Hence

$$C = \theta C_L + \rho(C_{S1} + C_{S2}), \quad (4)$$

101 where C_{S1} and C_{S2} are the concentrations of fast- and slow-reacting U (per unit whole soil mass)
 102 and ρ is the soil bulk density. Therefore,

$$\frac{\partial C}{\partial t} = \theta \frac{\partial C_L}{\partial t} + \rho \left(\frac{\partial C_{S1}}{\partial t} + \frac{\partial C_{S2}}{\partial t} \right). \quad (5)$$

103 For the fast-reacting U,

$$\frac{\partial C_{S1}}{\partial t} = \frac{\partial C_{S1}}{\partial C_L} \frac{\partial C_L}{\partial t} = b \frac{\partial C_L}{\partial t}, \quad (6)$$

104 where the derivative b is the buffer power for the solid–solution distribution of fast-reacting U,
 105 which is a function of pH and CO_2 pressure (Boghi *et al.*, 2018, Equations 1–7; next section). For
 106 the slowly-reacting U, we assume reversible first-order kinetics (Boghi *et al.*, 2018, Equation 8):

$$\frac{dC_{S2}}{dt} = k_1 C_{S1} - k_2 C_{S2}, \quad (7)$$

107 where k_1 and k_2 are forward and backward rate constants. In Equation (1),

$$D \frac{\partial C}{\partial x} = D \frac{\partial C}{\partial C_L} \frac{\partial C_L}{\partial x} = D_L \theta f \frac{\partial C_L}{\partial x}. \quad (8)$$

108 Combining Equation (1) with Equations (5)–(8) and rearranging gives

$$(\theta + \rho b) \frac{\partial C_L}{\partial t} = \frac{\partial}{\partial x} \left(D_L \theta f \frac{\partial C_L}{\partial x} \right) - \rho (k_1 C_{S1} - k_2 C_{S2}). \quad (9)$$

109 *Equations for U speciation and fast sorption.* In our experimental system, the soil contains Ca^{2+} ,
 110 H^+ , H_2CO_3 , HCO_3^- , CO_3^{2-} , Cl^- and L^- (representing organic ligands) in the soil solution and Ca^{2+} in
 111 the soil exchange complex, in addition to U. Over the range of pH, P_{CO_2} and dissolved U
 112 concentration in our experiments, the important U species in solution are UO_2^{2+} , UO_2CO_3 ,

113 $\text{Ca}_2\text{UO}_2(\text{CO}_3)_3$ and $\text{CaUO}_2(\text{CO}_3)_3^{2-}$ (Figure S1, Supporting Information, gives speciation
 114 calculations) and to a lesser extent UO_2L^+ ; the solution is under-saturated with respect to known U
 115 minerals. The total concentration of U species in the soil solution is therefore:

$$C_L = [\text{UO}_2^{2+}]_L + [\text{UO}_2\text{CO}_3]_L + [\text{Ca}_2\text{UO}_2(\text{CO}_3)_3]_L + [\text{CaUO}_2(\text{CO}_3)_3^{2-}]_L + [\text{UO}_2\text{L}^+]_L =$$

$$[\text{UO}_2^{2+}]_L \left\{ 1 + K_{\text{UO}_2\text{CO}_3}[\text{CO}_3^{2-}]_L + K_{\text{Ca}_2\text{UO}_2(\text{CO}_3)_3}[\text{Ca}^{2+}]_L^2[\text{CO}_3^{2-}]_L^3 + \right.$$

$$\left. K_{\text{CaUO}_2(\text{CO}_3)_3^{2-}}[\text{Ca}^{2+}]_L[\text{CO}_3^{2-}]_L^3 + K_{\text{UO}_2\text{L}^+}[\text{L}^-]_L \right\}, \quad (10)$$

116 where the K terms are the respective conditional equilibrium constants adjusted for activity
 117 coefficients.

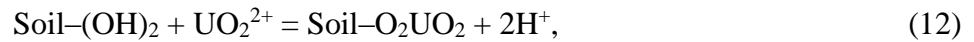
118 The unknowns in Equation (10) are $[\text{UO}_2^{2+}]_L$, $[\text{CO}_3^{2-}]_L$ and $[\text{Ca}^{2+}]_L$. The $[\text{CO}_3^{2-}]_L$ is defined by
 119 the pH and CO_2 pressure, and $[\text{Ca}^{2+}]_L$ is defined by the electrical neutrality condition:

$$2[\text{Ca}^{2+}]_L + 2[\text{UO}_2^{2+}]_L + [\text{UO}_2\text{L}^+]_L + [\text{H}^+]_L =$$

$$[\text{Cl}^-]_L + [\text{HCO}_3^-]_L + [\text{L}^-]_L + 2[\text{CaUO}_2(\text{CO}_3)_3^{2-}]_L \quad (11)$$

120 We assume the concentration of the balancing anion Cl^- is constant, it being far greater than the
 121 concentrations of other anions, and that the pH is constant, which is justified by the results of Boghi
 122 *et al.* (2018) who showed that acid–base changes in U sorption reactions have a negligible effect on
 123 the soil pH.

124 For the fast sorption reactions, Boghi *et al.* (2018) used the generalized surface complexation
 125 model of Davis *et al.* (2004) which gives semi-empirical equations for U sorption on soils and
 126 sediments. From a sensitivity analysis of Davis *et al.*'s equations, the generally-observed
 127 dependence of U sorption on soil pH and CO_2 pressure over the relevant ranges in our experiments
 128 was best described with the following two reactions:



129 and the corresponding two mass-action equilibrium equations:

$$\frac{C_{\text{S11}}[\text{H}^+]_L^2}{X_{\text{S1}}[\text{UO}_2^{2+}]_L} = K_{\text{S,UO}_2^{2+}}, \quad (14)$$

$$\frac{C_{\text{S12}}[\text{OH}^-]_L^2}{X_{\text{S1}}[\text{CaUO}_2(\text{CO}_3)_3^{2-}]_L} = K_{\text{S,CaUO}_2(\text{CO}_3)_3^{2-}}, \quad (15)$$

130 where $C_{\text{S11}} = [\text{Soil}-\text{O}_2\text{UO}_2]_s$, $C_{\text{S12}} = [\text{Soil}-\text{CaUO}_2(\text{CO}_3)_3]_s$, $X_{\text{S1}} = [\text{Soil}-(\text{OH})_2]_s$, the K_{SS} are
 131 conditional equilibrium constants and

$$C_{S11} + C_{S12} + X_{S1} = C_{S1} + X_{S1} = S1 \quad (16)$$

132 in which S1 is a constant. Therefore, for a given soil pH and CO₂ pressure and total fast-reacting U
 133 concentration, we have five unknowns: C_L, [UO₂²⁺]_L, [CaUO₂(CO₃)₃²⁻]_L, C_{S1} and X_{S1}. These are
 134 found with Equations (4), (10) and (14)–(16). This defines the buffer power *b* in Equation (6).

135 *Solution of the equations.* We solved Equation (9) subject to the initial and boundary conditions and
 136 the other equations using the Crank–Nicolson finite-difference method. Copies of the program,
 137 written in FORTRAN, are available (Supporting Information). The total soil U concentration and
 138 the values of pH, CO₂ pressure, [Cl⁻]_L, [L⁻]_L, ρ and θ are known from the experimental set up. The
 139 value of *f* is obtained from Br⁻ diffusion as below, and S1 is estimated from values of Davis *et al.*
 140 (2004). The following parameters were fitted to the data: $K_{S,UO_2^{2+}}$, $K_{S,CaUO_2(CO_3)_3^{2-}}$, k_1 and k_2 . The
 141 fitting was done using the *fmincon* function in MATLAB's Optimization Toolbox to optimize
 142 agreement between the measured and predicted concentration-distance profiles. A unique set of
 143 parameters for the whole dataset was found through a fitting algorithm, which minimizes the
 144 average of the fitting errors calculated for the individual replicate runs. We assessed the global error
 145 as

$$146 \quad E = \frac{1}{N} \sum_{i=1}^N |C_i^{\text{measured}} - C_i^{\text{modelled}}|$$

147 for the *N* experimental treatments × replicates (*N* = 15 given the six treatments and replicates
 148 analysed, Figures S3–S5, Supporting Information).

149 *Bromide diffusion*

150 We measured the diffusion of Br⁻ ions in our experimental system to confirm that the system
 151 behaves as expected from theory. Because Br⁻ ions are not adsorbed on the soil solid, the diffusion
 152 coefficient in the soil is constant and only influenced by tortuosity of the pore space therefore the
 153 complications of concentration- and time-dependency are avoided. Consequently the solution of the
 154 diffusion equation (Equation 1) subject to the boundary conditions in the half-cell system (Equation
 155 3) has the simple form (Crank, 1975, Equation 2.14)

$$\frac{C - C_0}{C_1 - C_0} = \frac{1}{2} \operatorname{erfc} \left(-\frac{x}{2\sqrt{Dt}} \right), \quad (17)$$

156 where *C* is the whole-soil concentration of Br⁻, subscripts 0 and 1 refer to the initial sink and source
 157 cells, respectively, *erfc* is the complimentary error function. For a non-adsorbed solute, $C = \theta C_L$
 158 and in Equation (2) $\theta dC_L/dC = 1$ and $D = D_L f$.

159 *Diffusion impedance factor*

160 We measured the diffusion impedance factor, f , under the conditions of the main experiments by the
161 method of Pinner & Nye (1982). A trace amount of a Br^- was deposited instantaneously on one end
162 of a column of soil prepared as for the main experiments, and the concentration-distance profile
163 measured (details below). The boundary conditions are

$$\begin{aligned} C = C_1 & \quad x = 0 & C = C_0 & \quad x > 0 & t = 0 \\ C = C_0 & \quad x = \infty & & & t \geq 0 \end{aligned} \quad (18)$$

164 where $x = 0$ is the source boundary and $x = \infty$ is the semi-infinite far-field boundary, and the
165 solution of Equation (1) subject to these conditions is (after Crank, 1975, Equation 2.7)

$$\frac{C - C_0}{C_1 - C_0} = \exp\left(-\frac{x^2}{4Dt}\right). \quad (19)$$

i.e.
$$\ln(C - C_0) = \ln(C_1 - C_0) + \exp\left(-\frac{x^2}{4Dt}\right) \quad (20)$$

166 Since $D = D_L f$ (last section), a graph of $\ln(C - C_0)$ against $x^2/4D_L t$ should have slope $-1/f$.

167 **Materials and methods**

168 Samples of topsoil (0–2-dm depth) of a typical brown earth (Wick series) were taken from Henfaes
169 Research Centre, Bangor University, Abergwyngregyn, Gwynedd, UK (53°14'24"N 4°01'33"W).
170 The soil was air-dried and sieved to < 0.5 mm after discarding large plant fragments. The properties
171 of the sieved soil were pH (in 10 mM CaCl_2) = 6.0, CEC (cation exchange capacity) = 1.02 cmol_c
172 kg^{-1} , organic C content = 30 g kg^{-1} , clay content = 145 g kg^{-1} , silt content = 328 g kg^{-1} . The soil was
173 washed three times with 10 mM CaCl_2 at a soil to solution ratio of 1:5, discarding the supernatant
174 after each washing, and then dried and re-sieved to < 0.5 mm.

175 *Uranium diffusion*

176 Quantities of soil with and without U at pH 6.0, 7.0 and 7.6 were prepared as follows. Samples of
177 air-dry soil were mixed with 150 mg kg^{-1} of ^{235}U -depleted uranium as uranyl nitrate (TAAB
178 Laboratories Equipment Ltd, Aldermaston, UK) at a soil to solution ratio of 2:1, and allowed to
179 equilibrate for 3 weeks. The soil was then air dried and re-sieved to < 0.5 mm. Samples of soil with
180 and without added U were mixed with amounts of $\text{Ca}(\text{OH})_2$ solution to adjust the soil pH (in 10 mM
181 CaCl_2) to 7.0 and 7.6, and allowed to equilibrate for 3 weeks before air-drying and re-sieving to <
182 0.5 mm.

183 Pre-weighed amounts of the air-dry soil were packed into 0.29-dm internal diameter, 0.3-dm
184 long Perspex cells to bulk density $\approx 1.4 \text{ kg dm}^{-3}$. To achieve uniform packing, the soil was poured
185 into the cells in stages, tapping down with pressure applied from above. The soil was then gradually
186 wetted from below with 10 mM CaCl_2 so that entrapped air was displaced, and it was then placed on
187 a pressure plate for 10 days at 55 kPa to bring the moisture content to $\theta \approx 0.35$. Preliminary tests in
188 which the soil was sectioned and the section weights and moisture contents determined showed that
189 this method produced uniform bulk densities and moisture contents to within 1 standard deviation
190 of the means. Two half-cells of soil were prepared, one with U and one without, with the same pH
191 in both cells (either pH 6.0, 7.0 or 7.6). The cells were joined and held together with tape to ensure
192 good inter-cell contact. They were then incubated at 20 °C in 16-L perspex boxes containing a
193 moisture-saturated atmosphere with either ambient or elevated P_{CO_2} maintained by passing a stream
194 of 5% CO_2 in air through the box at $0.05 \text{ L minute}^{-1}$. The P_{CO_2} in the soil air was measured in cells
195 incubated in this way (next section). The values were $P_{\text{CO}_2} = 1.3 \pm 0.1$ and 6.5 ± 0.1 kPa in the
196 ambient and elevated CO_2 treatments, respectively, and approximately constant along the length of
197 the cells. Three replicate runs were made for each pH and P_{CO_2} combination.

198 After 12 days, the cells were separated, frozen in liquid nitrogen and sectioned at approximately
199 0.5-mm intervals parallel to the inter-cell boundary using a microtome (Griffin and George DIEH
200 600-B) and a stainless steel blade. A total of approx. 0.1 dm of each cell was sectioned. The
201 thicknesses of the sections were calculated from their weights and the soil bulk density. The
202 sections were dried at 105 °C for 24 hours and then U extracted by placing them in 8 mL of aqua
203 regia (3:1 concentrated $\text{HCl}:\text{HNO}_3$) in a closed vessel overnight, and then digesting in a microwave
204 digester (Anton Paar Multiwave 3000). The digests were filtered (Whatman 542 filters), made up to
205 100 mL with ultra-pure water, and stored at 4°C until their U contents were analysed by inductively
206 coupled plasma mass spectroscopy (ICP–MS) as follows.

207 Samples were diluted with 0.3% aqua regia (Aristar grade) at 1:10 to reduce matrix effects, and
208 analysed using an Agilent 7500ce ICP–MS (Santa Clara, CA, USA), with rf forward power 1540 W
209 and reflected power 1 W, and Ar gas flows of $0.81 \text{ L minute}^{-1}$ and $0.19 \text{ L minute}^{-1}$ for carrier and
210 makeup flows, respectively. Solutions were aspirated by a micro-mist nebuliser at a rate of 1.2 mL
211 minute^{-1} . The instrument was operated in spectrum acquisition mode. Three replicate measurements
212 were taken per sample. Standards were prepared from a single element stock solution ($1000 \mu\text{g U L}^{-1}$,
213 PlasmaCal, SCP Science, Quebec, Canada) diluted with 0.3% aqua regia to $0.1\text{--}1000 \mu\text{g U L}^{-1}$.
214 An external calibration reference was prepared from Multi-Element Solution VI (Merck,
215 Kenilworth, NJ, USA) diluted 100-fold to give $100 \mu\text{g U L}^{-1}$. The extraction efficiency of this

216 method was close to 100% as measured by digesting a certified reference soil (IRMM; ERM-
217 CC141).

218 *CO₂ pressure in the soil air*

219 Triplicate half-cells of soil were prepared and incubated as for the main experiments in 16 L
220 perspex boxes containing a moisture-saturated atmosphere with either ambient or elevated P_{CO_2}
221 maintained by passing a stream of 5% CO₂ in air through the box at 0.05 L minute⁻¹. After 48 hours,
222 the cells were sliced axially into five sections and dissolved CO₂ in the soil solution measured as
223 follows. Approximately 5-g subsamples of each section were placed in centrifuge filtration units
224 (Millipore Ultrafree Centrifugal Filter Device (Burlington, MA, USA) with a 0.22- μm membrane),
225 capped and then centrifuged at 4000 g for 15 minutes, and the soil solution collected. Dissolved
226 CO₂ concentrations in the soil solutions were measured within a few minutes of collection using a
227 micro-electrode (MI-720 electrode, Microelectrodes Inc, Bedford, NH, USA). Preliminary
228 experiments showed the solution pH did not change over the few minutes between sampling and
229 analysis, indicating no degassing of dissolved CO₂. Calibration solutions (0.25–10 % CO₂) were
230 prepared by dissolving NaHCO₃ in CO₂-free ultra-pure water.

231 *Bromide diffusion*

232 Half-cells of soil were prepared as above, one containing Br and the other not. The Br addition was
233 made by moistening the cell with 0.1 mM CaBr₂ in 10 mM CaCl₂ when initially wetting the soil
234 before bringing it to the target moisture content on a pressure plate. The two half cells were joined
235 together and incubated in a moisture-saturated atmosphere at 20 °C for 4 hours. The cells were then
236 sectioned as above and Br concentrations analysed by shaking the sections end-over-end for 30
237 minutes with 0.01 M CaCl₂ at 1:10 soil:solution ratio, centrifuging the resulting suspensions at 3500
238 g for 10 minutes, filtering (0.45 μm filters) and measuring Br in the filtrates by ICP–MS
239 (PerkinElmer NexION 350, Boston, MA, USA). Three replicate runs were made.

240 *Diffusion impedance factor*

241 Cells of soil prepared as above were pulse-labelled with a trace amount of Br⁻ by placing a piece of
242 cellulose acetate membrane containing 4.7×10^{-6} mol of CaBr₂ in 10 mM CaCl₂ against one end of
243 the cell. After 5 minutes the membrane was removed, and the cell was incubated at 20 °C for 2
244 hours to allow the Br pulse to diffuse into the soil. The soil was then sectioned parallel to the $x = 0$
245 plane and the sections analysed for Br as above. The results were plotted as $\ln C$ against $x^2/4D_Lt$, and
246 Equation (19) was fitted iteratively, progressively rejecting data far from $x = 0$ until all the
247 remaining data agreed with the fitted values to within two standard deviations (Matschullat *et al.*,

248 2000). The fits to Equation (19) were made linear regression routines in SigmaPlot 11.0 (Systat
249 Software Inc, Chicago, IL, USA).

250 *Uranium sorption in shaken soil suspensions*

251 Solutions of 0, 10, 12, 24, 36, 48 and 60 mg U L⁻¹ in 10 mM CaCl₂ were made using uranyl nitrate.
252 Aliquots (2.5 cm³) of the solutions were added to 1 g of air-dry soils, prepared as under *Uranium*
253 *diffusion*, in 12 cm³ glass tubes. The tubes were capped with gas-tight rubber septa, and, in half of
254 them, the headspace air was displaced with 5% CO₂ in air by passing the gas through the tubes at 1
255 L minute⁻¹ for 30 s. In preliminary tests, in which the headspace was sampled and analysed by gas
256 chromatography, this was shown to provide a constant CO₂ pressure for the 24-hour duration of the
257 sorption measurements. The tubes were shaken end-over-end for 24 hours at 20 °C, after which the
258 suspension pHs were measured with a combination electrode. The suspensions were centrifuged at
259 3500 g for 10 minutes and filtered (0.45 µm filters), and U concentrations in the filtrates measured
260 as above. The amounts of U sorbed were inferred from the amounts added less the amounts
261 remaining in solution.

262 **Results and discussion**

263 *Bromide diffusion*

264 Figure 2a shows a plot of lnC against $x^2/4D_Lt$ for a pulse application of Br⁻ ions on the soil in accord
265 with Equation (19). From the slope, the diffusion impedance factor under the conditions of the main
266 experiments was $f = 0.39$ (sd < 0.01, $n = 2$). Figure 2b shows concentration-distance profile of Br⁻
267 ions in the half-cell system used in the main experiments and corresponding predictions of Equation
268 (17) using $f = 0.39$. The close agreement between the measured and theoretical profiles,
269 independently predicted, is strong evidence that the half-cell method is sound.

270 *Uranium diffusion*

271 *Model parameter values.* The values of D_L for the U species were calculated with the Stokes–
272 Einstein equation and the individual hydrated radii, giving for UO₂²⁺, UO₂CO₃, Ca₂UO₂(CO₃)₃ and
273 CaUO₂(CO₃)₃²⁻ $D_L = 7.60, 6.70, 4.60$ and 5.10×10^{-8} dm² s⁻¹, respectively (these are comparable to
274 published values of Kerisit & Liu, 2010). The values of the equilibrium constants for solution
275 speciation were taken from MINTEQ 3.0 (Gustafsson, 2013), adjusted for ionic strength using the
276 Davies equation. From the experimental set up, $\rho = 1.4 \pm 0.01$ kg dm⁻³ (soil), $\theta = 0.35 \pm 0.01$, $f =$
277 0.39 (last section), $[Cl^-]_L = 20$ mM, pH = 6.0, 7.0 or 7.6 and $P_{CO_2} = 1.3$ or 6.5 kPa. We set $[L^-]_L =$
278 0.1 mM based on typical concentrations of metal-chelating organic anions in soil solutions of
279 mineral soils (Jones *et al.*, 2003); at the pHs and P_{CO_2} values of our experiments, the model

280 predictions were not sensitive to this value (Boghi *et al.*, 2018). We set $S_1 = 5 \text{ mmol kg}^{-1}$ based on
281 values in Davis *et al.* (2004); this is equivalent to 50 % of the soil CEC. The addition of U to the
282 soil was 150 mg U kg^{-1} ($\equiv 0.63 \text{ mmol U kg}^{-1}$). The following parameters were fitted to the data:

283 $K_{\text{S,UO}_2^{2+}} = 2.30 \times 10^{-3} \text{ mol dm}^{-3}$ (solution), $K_{\text{S,CaUO}_2(\text{CO}_3)_3^{2-}} = 7.34 \times 10^{19} \text{ mol dm}^{-3}$ (solution), $k_1 = 6.95$
284 $\times 10^{-6} \text{ s}^{-1}$ and $k_2 = 9.39 \times 10^{-7} \text{ s}^{-1}$.

285 The values of the buffer power $b = dC_{\text{S}_1}/dC_{\text{L}}$, calculated with Equations 4, 10 and 14–16, are
286 6.03×10^4 , 180 and $5 \text{ dm}^3 \text{ kg}^{-1}$ at pH 6.0, 7.0 and 7.6 and $P_{\text{CO}_2} = 1.3 \text{ kPa}$, respectively, and $1.79 \times$
287 10^4 , 129 and $3 \text{ dm}^3 \text{ kg}^{-1}$ at $P_{\text{CO}_2} = 6.5 \text{ kPa}$, respectively (Figure 3). The buffer powers obtained in
288 shaken soil suspensions show the same trends with pH and P_{CO_2} (Figure 4), but the values are
289 different: $b = dC_{\text{S}}/dC_{\text{L}} = nmC_{\text{L}}^{n-1}$ (where m and n are Freundlich coefficients fitted to the data) =
290 5.74×10^3 , 428 and $10 \text{ dm}^3 \text{ kg}^{-1}$ at pH 6.0, 7.0 and 7.6 and ambient P_{CO_2} , respectively, and $5.21 \times$
291 $10^3 \text{ dm}^3 \text{ kg}^{-1}$, 60 and $6 \text{ dm}^3 \text{ kg}^{-1}$ at $P_{\text{CO}_2} = 6.5 \text{ kPa}$, respectively.

292 At equilibrium, $dC_{\text{S}_2}/dt = 0$ and from Equation (7), $k_1C_{\text{S}_1} = k_2C_{\text{S}_2}$. Therefore, since
293 $\rho(C_{\text{S}_1} + C_{\text{S}_2}) \gg \theta C_{\text{L}}$ (equilibrium $C_{\text{L}} = 0.06$, 1.2 and $48.2 \text{ }\mu\text{M}$ at pH = 6.0, 7.0 and 7.6 and $P_{\text{CO}_2} =$
294 1.3 kPa , and 0.09, 8.0 and $69.9 \text{ }\mu\text{M}$ at $P_{\text{CO}_2} = 6.5 \text{ kPa}$), the fraction of total U that is reacting slowly
295 is $C_{\text{S}_2}/(C_{\text{S}_1} + C_{\text{S}_2}) = 1/(1 + k_2/k_1) = 0.88$, i.e. the majority of the U in the soil.

296 *Concentration-distance profiles.* Figure 5 shows the measured U concentration-distance profiles at
297 the three pHs and two CO_2 pressures studied, compared with the model predictions, and Table 2
298 shows the amounts of U transferred between the half-cell couples, calculated from the amounts
299 accumulated in the sink cells. Replicate profiles (Figures S3–S5, Supporting Information) agreed
300 very well. As predicted by the model, there was little diffusion of U at pH = 6, but rates increased
301 steeply as both the pH and P_{CO_2} increased. The 5-fold increase in P_{CO_2} between the experimental
302 treatments caused a 2.8-fold increase in U transferred at pH 7.0 and a 1.8-fold increase at pH 7.6.

303 A striking finding was the discontinuity in the concentration-distance profiles at the inter-cell
304 boundary, $x = 0$. A possible explanation is that there was poor contact between the cells, resulting in
305 a boundary layer resistance. Crank (1975, Section 3.4) showed how such an interface resistance
306 would be expected to produce discontinuities in concentration-distance profiles, and that the effect
307 would increase as Dt decreases (Crank, 1975, Fig. 3.7). The value of Dt for Br^- diffusion in our
308 experimental system ($= 1.1 \times 10^{-3} \text{ dm}^2$) was comparable to that for U diffusion at pH 7.6 ($= 0.8$ and
309 $1.4 \times 10^{-3} \text{ dm}^2$ at $P_{\text{CO}_2} = 1.3$ and 6.5 kPa , respectively). Therefore, the smooth profiles we obtained
310 for Br^- diffusion (Figures 2b and S2, Supporting Information), and the close agreement of these

311 profiles with theory, showed that there was no interface resistance. We therefore reject this
312 explanation.

313 Rather we consider the discontinuity to be due to slow equilibration of diffusing U between the
314 soil solution and soil solid, as predicted by the model. Because there is no interface resistance, the
315 concentrations of U in the soil solution on either side of the boundary must be equal. However, if
316 the interchange of U between the soil solid and solution is slow compared with diffusion, the
317 whole-soil U concentration will lag behind the soil solution concentration leading to an abrupt
318 change between the source cell, where U is desorbing from the soil solid, and the sink cell, where it
319 is being adsorbed.

320 The half-time for slow equilibration is $t_{1/2} = \ln 2/k_2 = 8.5$ days. Boghi *et al.* (2018) showed that
321 slow equilibration will increasingly affect rates of U diffusion in soil for $k_2 < 10^{-6} \text{ s}^{-1}$ (i.e. $t_{1/2} > 8$
322 days). Such rates are reported in the literature (Braithwaite *et al.*, 1997; Qafoku *et al.*, 2005;
323 Handley-Sidhu *et al.*, 2009). The published measurements are, however, mostly from shaken
324 suspension or column leaching experiments in which sorption is artificially accelerated by
325 convection and, in shaken suspensions, disaggregation of the soil, exposing sorption sites that are
326 otherwise accessed only slowly by intra-aggregate diffusion (Nye & Staunton, 1994; Ptashnyk *et*
327 *al.*, 2010). The kinetics inferred from our experimental system, in which the soil solution is
328 stationary, are more reliable. Further, we have measured the kinetics of both adsorption, which is
329 what is usually measured, and desorption, which is what is needed for modelling diffusion to a sink,
330 such as a plant root.

331 The extent of sorption is a function of pH and P_{CO_2} because they affect both U speciation in
332 solution and the soil surface charge. Boghi *et al.* (2018) considered only sorption of the uranyl
333 cation, UO_2^{2+} , by the soil solid (Equation 12). However at the high pH and CO_2 pressures of our
334 experimental system, we also found? it is necessary to allow for sorption of the $\text{CaUO}_2(\text{CO}_3)_3^{2-}$
335 anion to account for our results. Otherwise, the decline in fast sorption (as represented by the buffer
336 power b in Equation 9) with pH above 6.0 is too steep.

337 *Sensitivity analysis*

338 Figure 6 shows the sensitivity of the inter-cell flux of U to the indicated parameters as they were
339 varied about the values used in Figure 5 with pH = 7.0. It shows that at this pH and the indicated
340 P_{CO_2} , the flux is sensitive to $K_{\text{S,CaUO}_2(\text{CO}_3)_3^{2-}}$ but not $K_{\text{S,UO}_2^{2+}}$ because UO_2^{2+} is unimportant compared
341 with $\text{CaUO}_2(\text{CO}_3)_3^{2-}$. It also shows that we are at the upper end of the P_{CO_2} range in which further
342 increases have an effect. Our P_{CO_2} values are at the upper end of the range found in freely-drained

343 soils (Greenway *et al.*, 2006). Soil P_{CO_2} varies with soil organic C content, root and microbial
344 activities, and soil moisture status because they affect both CO_2 generation and its escape by
345 diffusion in the soil air. Therefore, values are generally at least an order of magnitude above
346 atmospheric P_{CO_2} . Likewise the predicted flux decreased as k_2 decreased below the standard value,
347 but was not sensitive to increases above the standard value. Changes in k_1 at constant k_2 did not
348 have much effect. As k_1 increased from 0.1 to $10 \times$ the standard value, the equilibrium distribution
349 of $U = C_{\text{S}_2} / (C_{\text{S}_1} + C_{\text{S}_2}) = 1 / (1 + k_2 / k_1)$ increased from 0.43 to 0.99. However, increases in k_1 would
350 not have much influence net adsorption, and so the flux across $x = 0$ – if $k_1 C_{\text{S}_1} \ll k_2 C_{\text{S}_2}$.

351 *Implications for U uptake by plants*

352 We have shown that U diffusion was slow at $\text{pH} < 6$ but increased steeply at $\text{pH} > 6$. Boghi *et al.*
353 (2018) showed that root-induced pH changes controlled by the plant's N nutrition are likely to be
354 important in this pH range. Ammonium (NH_4^+) fed plants tend to acidify their rhizosphere, and this
355 would tend to diminish U uptake. Nitrate (NO_3^-)-fed plants, however, make their rhizosphere more
356 alkaline, and this would increase U uptake. The change in pH was often as much as one unit, but
357 was sensitive to the initial pH and CO_2 pressure (Boghi *et al.*, 2018).

358 The importance of slow equilibration shown by our results has the obvious implication that it is
359 important to allow for it correctly in modelling U uptake. Slow equilibration has the effect of
360 decreasing the diffusive flux to a sink such as a plant root. An implication of this is that plants with
361 fast growing root systems will accumulate more U over time than ones with slow growing roots.
362 Such effects will also depend on the geometry of the root system and the proportions of fine roots
363 and root hairs because these affect the spread of depletion profiles.

364 **Conclusions**

- 365 1. Measurements of U sorption kinetics in shaken soil suspensions were compromised by the
366 effects of convection and disaggregation of the soil, exposing otherwise only slowly-accessible
367 sorption sites.
- 368 2. Reaction kinetics inferred from concentration-distance profiles in soil columns with the soil
369 solution stationary, as here, were more realistic.
- 370 3. The numerical model developed here, allowing for the effects of concentration, pH, CO_2
371 pressure and time on U adsorption and desorption, correctly predicted the measured U
372 concentration-distance profiles.
- 373 4. Because all the model parameters were measured or otherwise estimated independently of the
374 concentration-distance profiles, this indicated that the model correctly accounted for all the
375 important processes.

376 5. A sensitivity analysis of the model indicated that the important effects to be allowed for in
377 modelling U uptake by plant roots were the effects of pH, CO₂ pressure and organic and
378 inorganic ligands on U speciation and sorption, and the effects of sorption kinetics.

379 **Supporting information**

380 A. Maximum U influx into roots because of mass flow.

381 **Table S1** Maximum U influx into roots due to mass flow.

382 B. Uranium speciation in solution.

383 **Figure S1.** Uranium speciation in solution.

384 C. Further results

385 **Figure S2.** Measured and calculated concentration-distance profiles of Br.

386 **Figure S3.** Measured and calculated concentration-distance profiles of U at pH 6.0.

387 **Figure S4.** Measured and calculated concentration-distance profiles of U at pH 7.0.

388 **Figure S5.** Measured and calculated concentration-distance profiles of U at pH 7.6.

389 Copies of the experimental data and the program for the model are available from

390 <https://doi.org/10.17862/cranfield.rd.7093574/>.

391 **Acknowledgements**

392 This research was funded by NERC, Radioactive Waste Management Ltd and the Environment
393 Agency through the Radioactivity and the Environment (RATE) programme (Grant Reference
394 NE/L000288/1, Long-lived Radionuclides in the Surface Environment (LO-RISE)) and we thank
395 Francis Livens and Gareth Law of the University of Manchester for leading the LO-RISE
396 Consortium.

397 **References**

- 398 Boghi, A., Roose, T. & Kirk, G. J. D. 2018. A model of uranium uptake by plant roots allowing for
399 root-induced changes in the soil. *Environmental Science & Technology*, 52, 3536–3545.
- 400 Braithwaite, A., Livens, F. R., Richardson, S., Howe, M. T. & Goulding K. W. T. 1997. Kinetically
401 controlled release of uranium from soils. *European Journal of Soil Science*, 48, 661–673.
- 402 Crank, J. 1975. *The Mathematics of Diffusion*, Second Edition. Oxford University Press, Oxford.
- 403 Davies, H. S., Cox, F., Robinson, C. H. & Pittman, J. K. 2015. Radioactivity and the environment:
404 technical approaches to understand the role of arbuscular mycorrhizal plants in radionuclide
405 bioaccumulation. *Frontiers in Plant Science*, 6, 580. doi: 10.3389/fpls.2015.00580.

406 Davis, J. A., Meece, D. E., Kohler, M. & Curtis, G. P. 2004. Approaches to surface complexation
407 modeling of Uranium (VI) adsorption on aquifer sediments. *Geochimica et Cosmochimica Acta*,
408 68, 3621–3641.

409 Duquène, L., Vandenhove, H., Tack, F., Van Hees, M. & Wannijn, J. 2010. Diffusive gradient in thin
410 films (DGT) compared with soil solution and labile uranium fraction for predicting uranium
411 bioavailability to ryegrass. *Journal of Environmental Radioactivity*, 101, 140–147.

412 Geckeis, H., Lützenkirchen, J., Polly, R., Rabung, T. & Schmidt, M. 2013. Mineral–water interface
413 reactions of actinides. *Chemical Reviews*, 113, 1016–1062.

414 Greenway, H., Armstrong, W. & Colmer, T. D. 2006. Conditions leading to high CO₂ (>5 kPa) in
415 waterlogged–flooded soils and possible effects on root growth and metabolism. *Annals of*
416 *Botany*, 98, 9–32.

417 Gustafsson, J. P. 2013. *Visual MINTEQUATION Version 3.0*. KTH, Stockholm.

418 Handley-Sidhu, S., Bryan, N. D., Worsfold, P. J., Vaughan, D. J., Livens, F. R. & Keith-Roach, M.
419 J. 2009. Corrosion and transport of depleted uranium in sand-rich environments. *Chemosphere*,
420 77, 1434–1439.

421 Jones, D. L., Dennis, P. G., Owen, A. G. & van Hees, P. A. W. 2003. Organic acid behavior in soils
422 – misconceptions and knowledge gaps. *Plant and Soil*, 248, 31–41.

423 Kerisit, S. & Liu, C. 2010. Molecular simulation of the diffusion of uranyl carbonate species in
424 aqueous solution. *Geochimica et Cosmochimica Acta*, 74, 4937–4952

425 Matschullat, J., Ottenstein, R. & Reimann, C. 2000. Geochemical background – Can we calculate
426 it? *Environmental Geology*, 39, 990–1000.

427 Mitchell, N., Pérez-Sánchez, D. & Thorne, M. C. 2013. A review of the behaviour of U-238 series
428 radionuclides in soils and plants. *Journal of Radiological Protection*, 33, R17–R48.

429 Nye, P. H. & Staunton, S. 1994. The self-diffusion of strongly adsorbed anions in soil: two-path
430 model to simulate restricted access to exchange sites. *European Journal of Soil Science*, 45,
431 145–152.

432 Pinner, A. & Nye, P. H. 1982. A pulse method for studying effects of dead-end pores, slow
433 equilibration and soil structure on solute diffusion in soil. *Journal of Soil Science*, 33, 25–35.

434 Ptashnyk, M., Roose, T. & Kirk, G. J. D. 2010. Diffusion of strongly sorbed solutes in soil: a dual-
435 porosity model allowing for slow access to sorption sites and time-dependent sorption reactions.
436 *European Journal of Soil Science*, 61, 108–119.

437 Qafoku, N. P., Zachara, J. M., Liu, C. X., Gassman, P. L., Qafoku, O. S. & Smith, S. C. 2005.
438 Kinetic desorption and sorption of U(VI) during reactive transport in a contaminated Hanford
439 sediment. *Environmental Science & Technology*, 39, 3157–3165.

440 Stoliker, D.L., Liu, C.X., Kent, D.B. & Zachara, J.M. 2013. Characterizing particle-scale
441 equilibrium adsorption and kinetics of uranium(VI) desorption from U-contaminated sediments.
442 *Water Resources Research*, 49, 1163–1177.
443

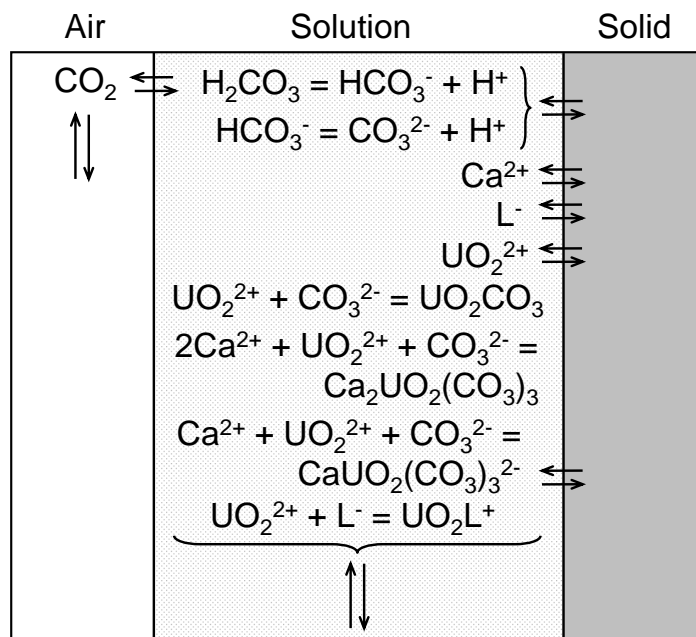
Symbol	Meaning	Units
C	concentration of U or Br in the whole soil	mol dm^{-3} (soil)
C_L	concentration of all U species in the soil solution	mol dm^{-3} (solution)
C_{S1}	concentration of fast-reacting U in the soil solid	mol kg^{-1} (solid)
C_{S2}	concentration of slow-reacting U in the soil solid	mol kg^{-1} (solid)
D	diffusion coefficient in soil	$\text{dm}^2 \text{s}^{-1}$
D_L	diffusion coefficient in free solution	$\text{dm}^2 \text{s}^{-1}$
f	diffusion impedance factor	
$[\text{ion}]_L$	concentration of ion in the soil solution where ion = U species, Ca^{2+} , L^- , Cl^-	mol dm^{-3} (solution)
$K_{S, \text{UO}_2^{2+}}$	equilibrium constant for fast sorption of UO_2^{2+} (Equation 14)	mol dm^{-3} (solution)
$K_{S, \text{CaUO}_2(\text{CO}_3)_3^{2-}}$	equilibrium constant for fast sorption of $\text{CaUO}_2(\text{CO}_3)_3^{2-}$ (Equation 15)	mol dm^{-3} (solution)
k_1, k_2	forward, backward rate constants for slow U sorption	s^{-1}
P_{CO_2}	CO_2 pressure in soil air	kPa
$S1$	concentration of fast-reacting U sorption sites in the soil solid	mol kg^{-1} (solid)
t	time	s
x	distance	dm
θ	soil volumetric moisture content	
ρ	soil bulk density	kg dm^{-3} (soil)

446 **Table 2** Amounts of U transferred between half-cell couples calculated from the amounts
447 accumulated in the sink cells in Figure 5. Data are means \pm standard errors ($n = 3$).

pH	U transferred ($\text{mol} \times 10^{-7}$)	
	$P_{\text{CO}_2} = 1.3 \text{ kPa}$	$P_{\text{CO}_2} = 6.5 \text{ kPa}$
6.0	0.75 \pm 0.07	0.90 \pm 0.07
7.0	3.84 \pm 0.74	10.80 \pm 1.87
7.6	15.10 \pm 1.46	24.50 \pm 8.29

448

449



450

451

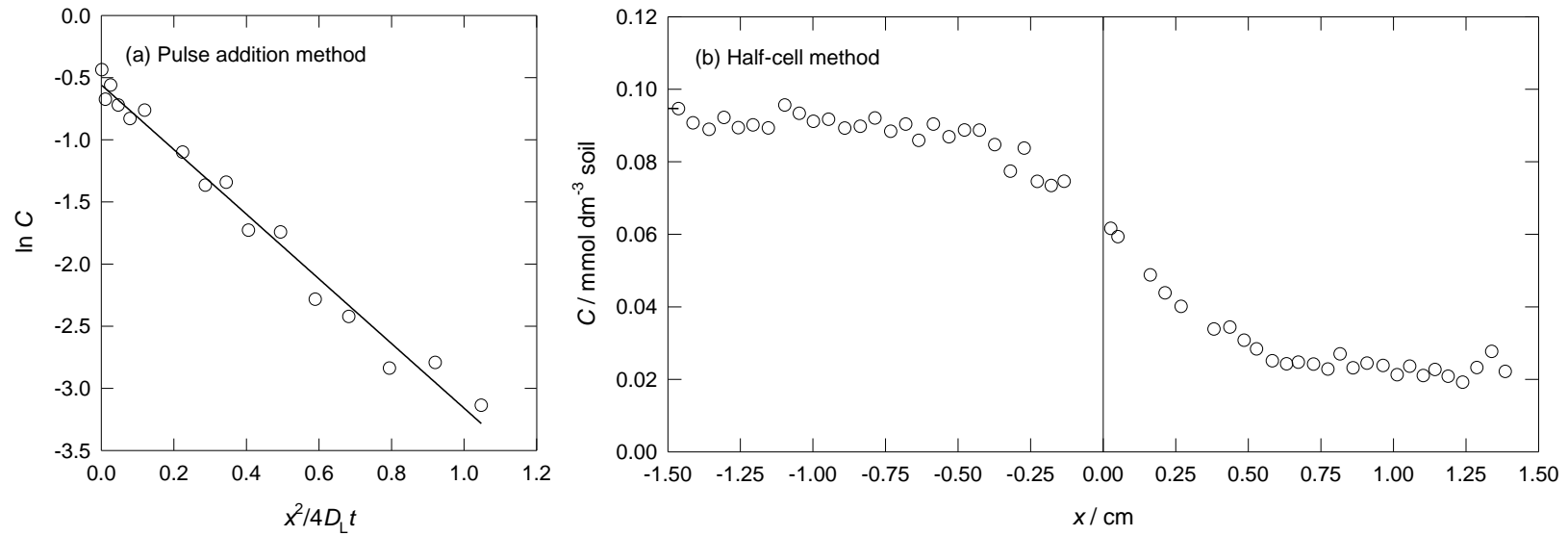
452

453

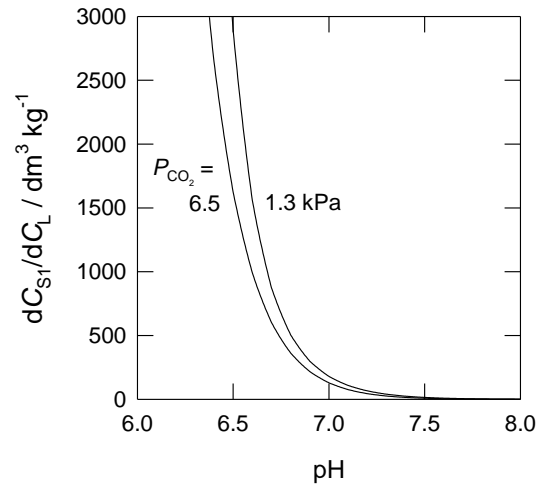
454

455

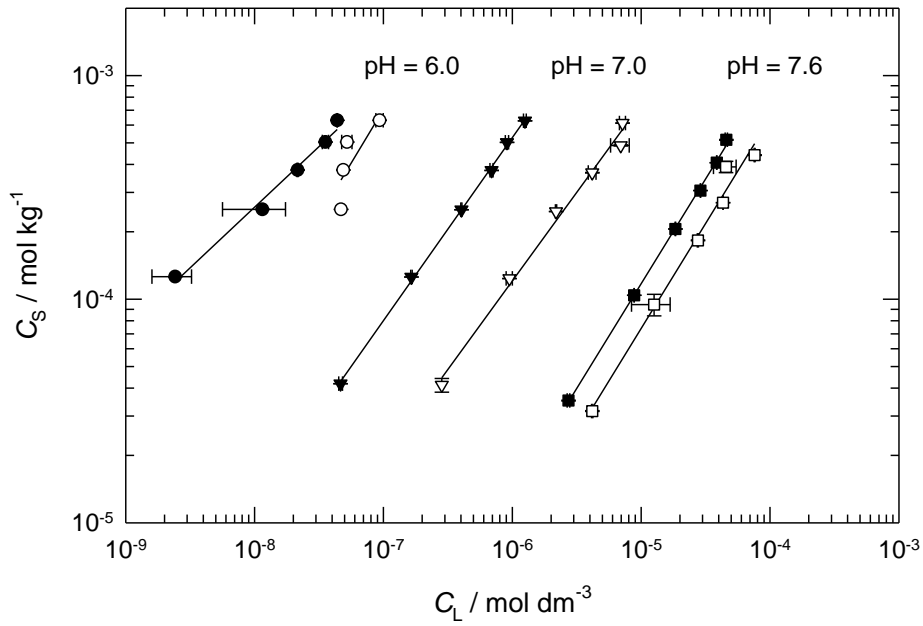
Figure 1 Speciation and sorption reactions controlling uranium diffusion in soil. Horizontal arrows indicate air–solution and solid–solution interchanges; vertical arrows indicate diffusion in the soil air and solution. Uranium species can diffuse in the soil solution but only very slowly in the soil solid.



456
 457 **Figure 2** Concentration-distance profiles for Br⁻ diffusion in the experimental soil under the conditions of the main experiment. (a) For a pulse addition
 458 of Br⁻ at one end of a soil cell ($x = 0$); the points are measured data and the line is the fit to Equation (19) giving $f = 0.39$. (b) For two half-cells of soil
 459 containing different initial concentrations of Br; the line is the fit to Equation (17) using $f = 0.39$. Soil bulk density, $\rho = 1.42 \text{ kg dm}^{-3}$; volumetric
 460 moisture content, $\theta = 0.36$; $D_L = 2.0 \times 10^{-7} \text{ dm}^2 \text{ s}^{-1}$.



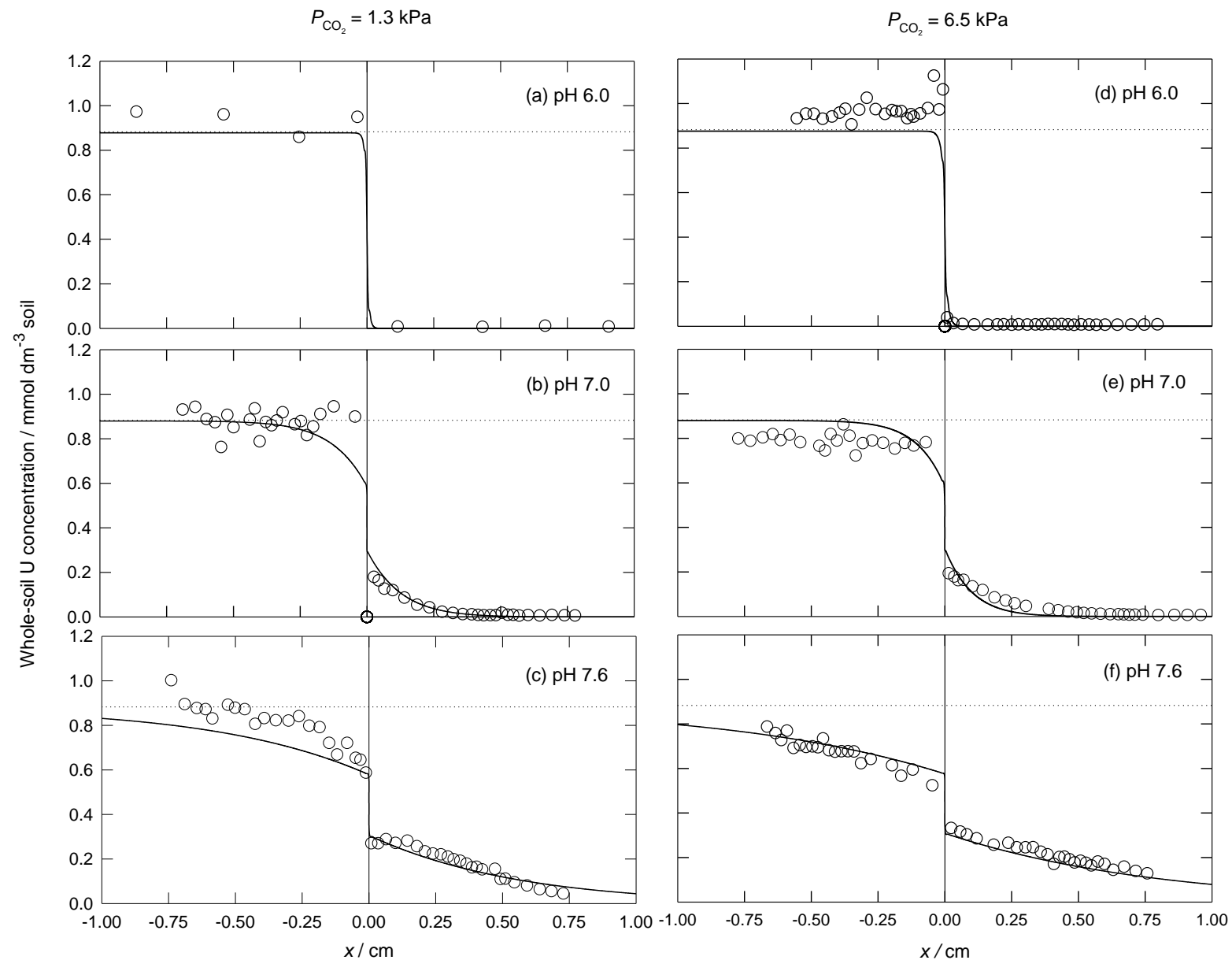
461
 462 **Figure 3** Effect of pH and P_{CO_2} on the buffer power $b = dC_{S1}/dC_L$ for fast U sorption.
 463



464

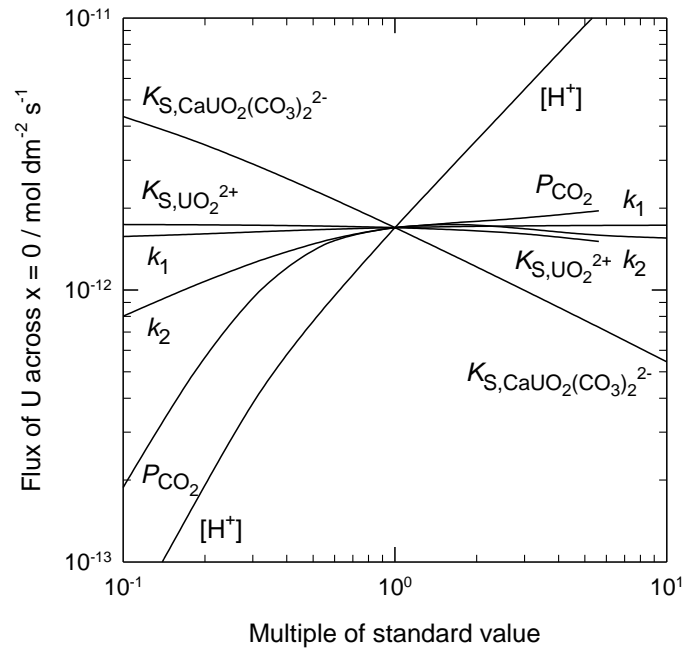
	Ambient air			5% CO ₂ in air		
	pH = 6.0	pH = 7.0	pH = 7.6	pH = 6.0	pH = 7.0	pH = 7.6
<i>m</i>	3.86	43.74	5.60	149.2	5.47	3.27
<i>n</i>	0.523	0.818	0.936	0.764	0.775	0.928
<i>R</i> ²	0.92	1.00	1.00	0.60	0.98	0.97

465 **Figure 4** Uranium sorption measured in shaken soil suspensions. Closed symbols are at ambient
 466 CO₂ pressure; open symbols at 5% CO₂ in air. Data are means ± SE; lines are fits of the data to $C_s =$
 467 mC_L^n with the coefficients *m* and *n* as shown in the table.



468

469 **Figure 5** Concentration-distance profiles of U after diffusion between two half-cells of soil, one initially with and the other without added U. Points are
 470 observed data for a single replicate (Figures S3–S5, Supplementary Information, show all replicates); solid lines are calculated with the model; dashed
 471 lines are added U. (a)–(c) P_{CO_2} (CO_2 pressure) = 1.3 kPa and indicated pHs. (d)–(f) P_{CO_2} = 6.5 kPa and indicated pHs.



472

473 **Figure 6** Sensitivity of the model to its input parameters. Each of the indicated parameters was
 474 varied in turn with the other parameters at their standard values. pH = 7.0; other standard parameter
 475 values as for Figure 4. $K_{S,UO_2^{2+}}$, $K_{S,CaUO_2(CO_3)_3^{2-}}$ = equilibrium constants for sorption of UO_2^{2+} ,
 476 $CaUO_2(CO_3)_3^{2-}$; k_1 , k_2 = forward, backward rate constants for slow U sorption; P_{CO_2} = CO_2 pressure
 477 in the soil air; $[H^+]$ = initial H^+ concentration in the soil solution.

Uranium diffusion and time-dependent adsorption–desorption in soil: a model and experimental testing of the model

Darmovzalova, Jana

2019-04-01

Attribution-NonCommercial 4.0 International

Darmovzalova J, Boghi A, Otten W, et al., (2020) Uranium diffusion and time-dependent adsorption–desorption in soil: a model and experimental testing of the model. *European Journal of Soil Science*, Volume 71, Issue 2, March 2020, pp. 215-225

<https://doi.org/10.1111/ejss.12814>

Downloaded from CERES Research Repository, Cranfield University